Integral Solution for the Mean Flow Profiles of Turbulent Jets, Plumes, and Wakes

Amit Agrawal
e-mail: agrawaa@me.udel.edu

Ajay K. Prasad
e-mail: prasad@me.udel.edu

Department of Mechanical Engineering,
University of Delaware,
Newark, DE 19716

Integral methods are used to derive similarity solutions for several quantities of interest including the cross-stream velocity, Reynolds stress, the dominant turbulent kinetic energy production term, and eddy diffusivities of momentum and heat for axisymmetric and planar turbulent jets, plumes, and wakes. A universal constant is evaluated for axisymmetric and planar plumes. The cross-stream velocity profiles show that jets and axisymmetric plumes experience an outflow near the axis and an inflow far away from it. The outflow is attributed to the decay of the centerline velocity with downstream distance, and the extent and magnitude of outflow correlates with the streamwise decay of the centerline velocity. It is also shown that the entrainment velocity should not in general be equated to the product of the entrainment coefficient and the centerline velocity. It is found that, due to similar governing equations, profiles for jets and plumes are qualitatively similar. Our results show that the derived quantities are strong functions of streamwise and cross-stream positions, in contrast to previous approaches that assumed constant (in the cross-stream direction) eddy viscosity and thermal diffusivity. The turbulent Prandtl number is approximately equal to unity which matches the value quoted in the literature.
[DOI: 10.1115/1.1603303]

Introduction

Jets, plumes, and wakes are examples of free shear flows. A jet is produced when fluid exits a nozzle with some initial momentum. On the other hand, plumes are driven purely by buoyancy addition at the source. Jets and plumes spread laterally by engulfing (entraining) ambient fluid. The momentum contained within the jet remains constant at any streamwise cross section, whereas the momentum contained within the plume increases monotonically with the streamwise coordinate while maintaining a constant buoyancy. The width of jets and plumes increases at the cost of velocity. Wakes are produced behind an object placed in a freestream, and manifest themselves in the form of a velocity deficit profile.

Jets, plumes, and wakes exhibit self-similarity beyond a certain downstream distance such that a characteristic length and velocity can be used to scale all distances and velocities in the flow. Analyses and measurements have traditionally focused on the self-similar region because fewer independent variables are involved making it is easier to interpret the results. For jets, plumes and wakes, the time-averaged centerline velocity is generally chosen as the characteristic velocity, the time-averaged centerline temperature differential (with respect to the ambient) is used as the characteristic temperature scale, whereas the cross-stream distances are scaled with the local width. Although more analysis is available for planar cases, it is somewhat easier to setup experimentally an axisymmetric jet, plume, or wake, compared to their planar counterparts. Consequently, more experimental data is available for the axisymmetric case, [1–5].

In the self-similar region of the flows under consideration, the traditional approach is to first perform an order of magnitude analysis of the Navier-Stokes equations. A boundary layer approximation is usually applied, allowing a substantial reduction in the number of terms. The resulting terms are then scaled using the appropriate length, velocity, and temperature scales. Further, by invoking conservation of momentum and buoyancy for jets and plumes, respectively, one can obtain the streamwise variation of width, centerline velocity and temperature, [6]. Because the number of unknowns exceeds the number of equations by one, the analysis fails to provide the cross-stream variation of these quantities. Of key interest is the functional form of the streamwise velocity in the cross-stream direction.

One approach to close the system of equations is to assume that the eddy viscosity (ν_T) is constant in the cross-stream direction, [6–10]. The equations are then solved to obtain the required functional form. With this approach, one obtains $U/U_c = \mathrm{sech}^2(A\xi)$ for a plane jet where $A=0.706$, and $(1+B\xi^2)^{-2}$ for a round jet where $B=0.661$, [7]. The intent of this paper is to follow the *opposite* approach, i.e., we select a functional form for the streamwise velocity profile based on experimental data to close the system of equations, and subsequently derive expressions for several useful quantities (including ν_T, which can show a cross-stream variation depending on the choice of the functional form).

Numerous experimental and numerical studies on free-shear flows have been undertaken by various groups in the past. Most of these studies measure (or compute) the streamwise velocity profile, and fit a simple mathematical expression to the data. The literature reveals that many researchers, [1–3,11–16] prefer the Gaussian function to approximate the streamwise velocity and temperature profiles. Our own measurements of axisymmetric jets also reveal that overall the Gaussian profile is a superior fit to the data. As an example, we plot in Fig. 1 the normalized streamwise velocity data for an axisymmetric jet of water issuing from a 2-mm orifice into a large tank; data were acquired using two-dimensional PIV at $110 \leqslant z/d \leqslant 175$ (see [17] for experimental details). The computed profile for Reynolds stress is compared with experimental measurements made by the authors later in the paper to provide additional validation for the choice of the Gaussian streamwise velocity profile. For these reasons, we preferred the Gaussian profile to the other choices as the input functional form for our analysis. Some previous researchers have employed an approach similar to ours to verify certain difficult measurements—for example, Wygnanski and Fiedler [5] and Gutmark and Wygnanski [18] verified their measurements of Reynolds stress against values computed from their streamwise velocity profile using an intergal approach.

Contributed by the Fluids Engineering Division for publication in the JOURNAL OF FLUIDS ENGINEERING. Manuscript received by the Fluids Engineering Division July 22, 2002; revised manuscript received May 6, 2003. Associate Editor: J. S. Marshall.

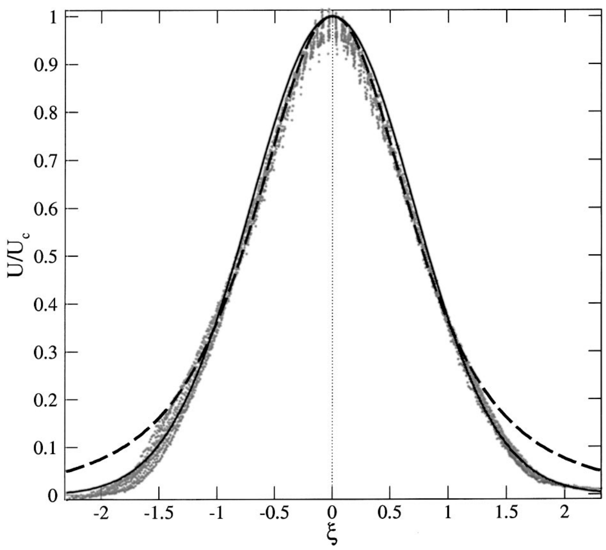

Fig. 1 Streamwise velocity profiles for jets (—— axisymmetric jet from Gaussian profile, -- axisymmetric jet from polynomial profile, [7], dots from experiment, [7]

Perhaps because the primary aim of these researchers was to verify measurements, they did not exploit integral theories to its full extent, nor did they discuss the properties of the expressions that they derived. In fact, explicit expressions for even basic quantities are not readily available in the literature. The aim of this paper is to extract a complete set of results from the integral method. We derive a host of useful expressions and explore their properties in physical terms. As we show, several interesting features of the flow can be obtained, and some probable misconceptions can be corrected in this manner. Further, upon contrasting appropriate solutions (for example jets versus plumes, axisymmetric versus planar), our approach yields some new insights.

The basic approach adopted here comprises the following three steps. First, we assume an analytical expression for the mean streamwise velocity U (and temperature). Second, the expression for U is substituted into the continuity equation along with the assumption of the centerline velocity variation, and integrated to determine the mean cross-stream velocity profile. Third, the expressions for U and V are substituted into the simplified momentum (and energy) equations, and integrated to determine the Reynolds stress (and velocity-temperature correlations). These expressions can then be employed to derive a number of useful quantities. Integral methods are shown here to be successful in reproducing experimental results for standard jets, plumes and wakes (axisymmetric and planar) which are commonly used as model flows in a variety of situations. Our results should serve as a useful reference for such studies. However, it should be remembered that integral methods may have restricted application to more complex turbulent flows, [13], where it is difficult to assign profile shapes, and relate entrainment rates to local influences in complex environments.

The relevant governing equations for jets and wakes are the continuity and the streamwise momentum equation. The two additional momentum equations, cross stream and azimuthal, relate pressure with the fluctuating components of velocity, and the fluctuating components of velocity with themselves, respectively; in this paper, we are not interested in exploring these relationships. For plumes, an additional equation for temperature is required. By symmetry considerations, both the cross-stream velocity and the Reynolds stress are zero at the centerline. We have used this condition throughout this paper to evaluate the constant of integration.

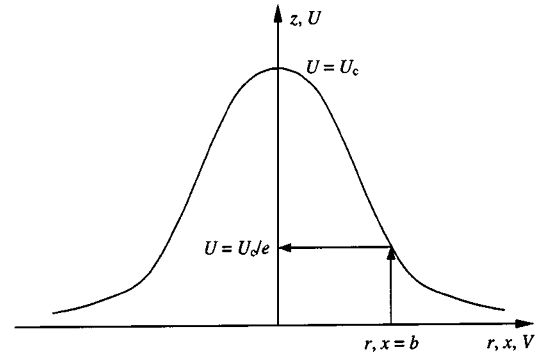

Fig. 2 Coordinate system for planar (x,z) and axisymmetric (r,z) jets, plumes, and wake. For wakes, U represents the velocity defect.

Turbulent Jets

Axisymmetric Jets. The continuity equation for the time-averaged velocities in cylindrical coordinates (see Fig. 2 for the coordinate system used in this paper) is

$$\frac{1}{r}\frac{\partial rV}{\partial r}+\frac{\partial U}{\partial z}=0. \tag{1}$$

In the self-similar region, the simplified streamwise momentum equation can be obtained using an order of magnitude analysis as, [6],

$$V\frac{\partial U}{\partial r}+U\frac{\partial U}{\partial z}+\frac{1}{r}\frac{\partial r\overline{uv}}{\partial r}=0 \tag{2}$$

where the overbar denotes time-averaged quantities.

For the self-similar axisymmetric jet, U_c varies as z^{-1}, while b increases linearly with z, [6]. By approximating the streamwise velocity at any downstream location by a Gaussian, [3,11–13,17], (see also Fig. 1)

$$\begin{aligned} U(r,z) &= U_c(z)\exp(-r^2/b^2(z)) \\ &= U_c(z)\exp(-r^2/c^2z^2) \\ &= U_c(z)\exp(-\xi^2), \end{aligned} \tag{3}$$

one can solve for V by substituting Eqs. (3) into (1):

$$\frac{V}{U_c}=\frac{c}{2\xi}(-1+\exp(-\xi^2)+2\xi^2\exp(-\xi^2)). \tag{4}$$

$V(\xi)/U_c$ is plotted in Fig. 3 and reveals that, contrary to the connotation of an inflow implied by the term ''entrainment,'' the cross-stream flow in the vicinity of the centerline is actually outward, i.e., $V(\xi)/U_c \geqslant 0$ for $0 \leqslant \xi \leqslant 1.12$. ($V(\xi)/U_c=0$ at the centerline, reaches a maximum of 0.018 at $\xi=0.54$ and declines back to zero at $\xi=1.12$.) The reason for such an outflow is that the centerline velocity decreases as z^{-1}, and *not* because of the Gaussian streamwise velocity profile assumption. $V(\xi)/U_c<0$ (i.e., inward) for $\xi>1.12$, reaches a minimum of -0.022 at $\xi=2.08$ and asymptotes to 0 as $\xi\to\infty$. It should be pointed out that $V\to 0$ much more slowly than U, i.e., although the central region is dominated by the axial component of velocity, the cross-stream flow predominates far away from it.

According to [11], the entrainment coefficient α can be defined using the incremental volume flux as

$$\frac{d\mu}{dz}=2\pi bU_c\alpha, \tag{5}$$

where μ for axisymmetric jets is given by

$$\mu=\int_0^\infty 2\pi rU(r)dr.$$

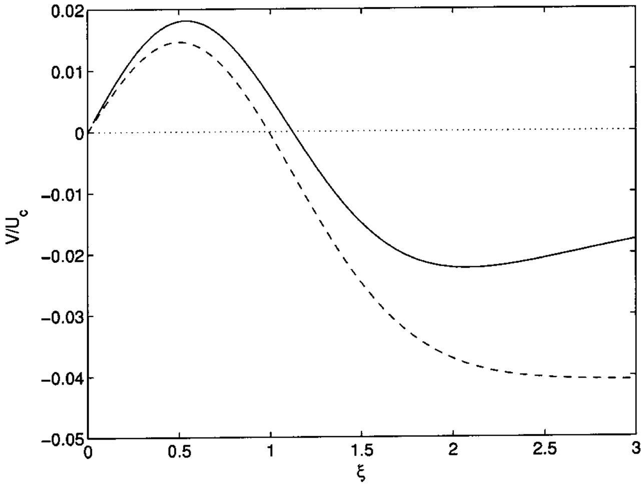

Fig. 3 Cross-stream velocity profiles for jets (—— axisymmetric jet, -- planar jet)

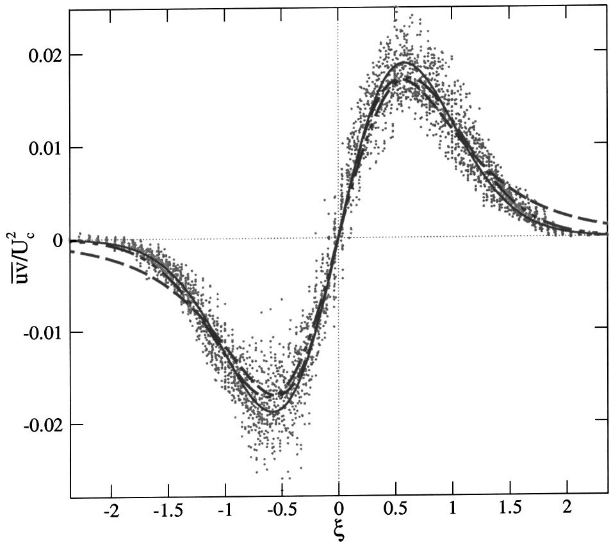

Fig. 4 Reynolds stress profiles for jets (—— axisymmetric jet from Gaussian profile, -- axisymmetric jet from polynomial profile, [7], -.. planar jet, dots from experiment)

It is readily seen that $d\mu/dz$ is the incremental volume flux entering the jet through a circular control surface at large r, i.e.,

$$\frac{d\mu}{dz}=\lim_{r\to\infty}-2\pi rV.$$

From Eq. (4), V/U_c for large ξ can be approximated as $-c/2\xi$. Our result gives

$$\frac{d\mu}{dz}=2\pi r\frac{c}{2\xi}U_c=2\pi bU_c\frac{c}{2}. \tag{6}$$

By equating Eqs. (5) and (6), we get $\alpha=c/2=0.0535$, which is the same value as obtained by [11]. From Fig. 3, it is seen that Turner's [11] statement: "the inflow velocity at the 'edge' of the flow is some fraction α of the maximum mean upward velocity," is not strictly correct, because V/U_c never reaches 0.0535 for any value of ξ. However, it is easily shown, [19], that the *inward extension* of the curve $c/2\xi$ (the asymptotic curve for V/U_c at large ξ) intersects the jet edge ($\xi=1$) with a value of $c/2$.

Equation (4) can also be derived using a control volume approach—by equating the difference of volume flux at two successive downstream stations to the incoming fluid volume. As seen in Fig. 3 the maximum value of V is just 2% of U_c, making it rather difficult to measure precisely, and therefore it is less frequently presented in the literature, [4,5].

The V profile can be used to directly determine the spread rate, c. Researchers in the past have determined c by curve fitting experimental data for U. However, determining c from the experimental profile for V may be advantageous since the location and height of the extrema can be unambiguously determined. However, as stated above, the experimental uncertainty in V can be substantial. (A comparison of the derived cross-stream velocity profile with the experimental data is provided in [20].)

One can insert the time-averaged profiles for U and V into Eq. (2), to obtain the time-averaged profile for Reynolds stress $\overline{uv}$ as

$$\frac{\overline{uv}}{U_c^2}=\frac{c}{2\xi}(\exp(-\xi^2)-\exp(-2\xi^2)). \tag{7}$$

The maximum for Reynolds stress lies at $\xi=0.58$ (Fig. 4). Wygnanski and Fiedler [5] provide a plot for Reynolds stress by integrating their streamwise velocity profile. However, they do not provide an explicit expression for it.

Figure 4 also shows our experimentally measured Reynolds stress for a (water) jet at Re=3000 using PIV. The experimental data can be compared with the analytical result based on the Gaussian profile and the one derived using the $(1+B\xi^2)^{-2}$ profile, [7], where $B=0.661$. We see that the latter result does not match as well, justifying the selection of the Gaussian profile for our analysis. Additionally, our analytical result matches very well with the Reynolds stress data of [5,18].

Planar Jets. It is worthwhile to compare the results for an axisymmetric jet against a planar jet. For planar jets the continuity and momentum equations are, respectively, [6]:

$$\frac{\partial V}{\partial x}+\frac{\partial U}{\partial z}=0, \tag{8}$$

$$V\frac{\partial U}{\partial x}+U\frac{\partial U}{\partial z}+\frac{\partial\overline{uv}}{\partial x}=0. \tag{9}$$

Like axisymmetric jets, plane jets have a linear spread rate and are well approximated by a Gaussian velocity profile, [13,15], (given again by Eq. (3) where ξ is now $x/b(z)$), but now the centerline velocity decays as $z^{-1/2}$, [6]. Integrating Eq. (8) using (3) we obtain

$$\frac{V}{U_c}=\frac{c}{4}(4\xi\exp(-\xi^2)-\sqrt{\pi}\,\mathrm{erf}(\xi)). \tag{10}$$

This expression has also been obtained by [15]. Similar to the axisymmetric case, we find an outflow near the jet axis, and an inflow far away from it. The maximum outflow occurs around $\xi=0.5$ (which is very close to the axisymmetric case) and the flow turns inward for $\xi\geqslant0.99$- this value is slightly smaller than for axisymmetric jets (Fig. 3).

Similar to the axisymmetric case we can define the coefficient of entrainment following Turner [11]:

$$\frac{d\mu}{dz}=2\alpha U_c, \tag{11}$$

where μ is now given by

$$\mu=\int_{-\infty}^{\infty}U\,dx.$$

Inserting Eq. (3) and differentiating with respect to z, we obtain

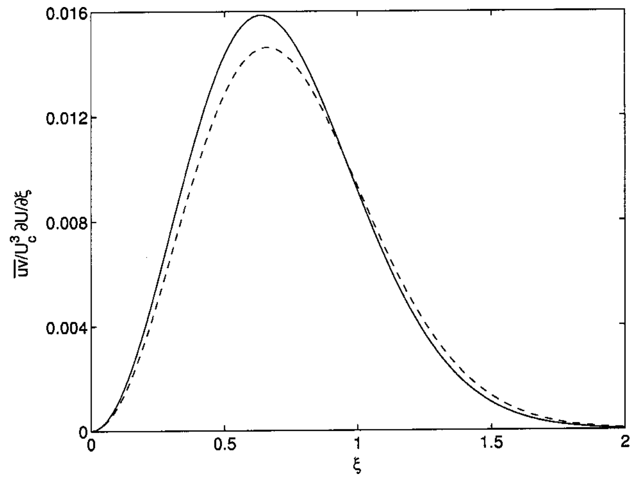

Fig. 5 Dominant kinetic energy production term profiles for jets (—— axisymmetric jet, -- planar jet)

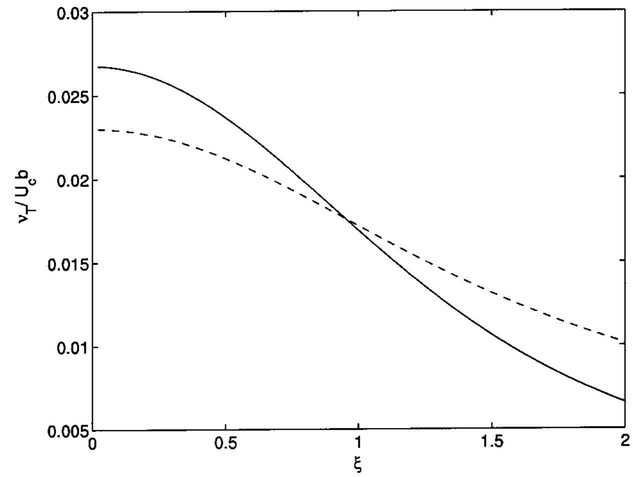

Fig. 6 Cross-stream variation of eddy viscosity for jets (—— axisymmetric jet, -- planar jet)

$$\frac{d\mu}{dz}=\frac{\sqrt{\pi}}{2}U_c c. \tag{12}$$

Equating Eqs. (11) and (12), we get $\alpha=\sqrt{\pi}c/4=0.041$ (from Fig. 5 of Gutmark and Wygnanski [18], we estimate $c=0.092$). It should be pointed out that the cross-stream velocity does become equal to αU_c for large ξ. Turner's [11] statement that the inflow velocity at the edge of the jet equals αU_c is thus seen to apply strictly in the case of planar free-shear flows.

Ramaprian and Chandrasekhara [15] measured α for planar jets as $\alpha=V_e/U_c=0.045$. The slight discrepancy might be due to the fact that their measurements, [15], were made rather close to the nozzle ($5\leqslant z/d\leqslant 60$) and therefore, the jet might not have achieved complete self-similarity.

As before, the momentum Eq. (9) along with the expressions for U and V can be used to solve for the Reynolds stress as

$$\frac{\overline{uv}}{U_c^2}=\frac{\sqrt{\pi}c}{4}\exp(-\xi^2)\mathrm{erf}(\xi). \tag{13}$$

The plot looks similar to that of axisymmetric jets with a maximum at $\xi=0.62$ and 0 for $\xi=0$ and large ξ (Fig. 4). In fact, the maxima lie at almost the same ξ and are of nearly the same magnitude. Although U profiles for the two cases considered above are similar, their V and the governing Eqs. (2) and (9) are very different. Thus it is not expected that $\overline{uv}$ would look so similar. This similarity is due to the fact that $U\partial U/\partial z$ is the dominating term, and behaves similarly for the two cases.

The dilution rates can be computed from

$$\frac{1}{\mu}\frac{d\mu}{dz}=\frac{c}{b}\quad\text{(axisymmetric jets)} \tag{14}$$

$$\frac{1}{\mu}\frac{d\mu}{dz}=\frac{c}{2b}\quad\text{(planar jets)}. \tag{15}$$

Because the spread rates for the two cases are virtually identical, it is obvious that axisymmetric jets dilute twice as rapidly as their planar counterparts (axisymmetric jets entrain circumferentially, while planar jets entrain from the two sides only). Greater mixing in the axisymmetric jets is consistent with the faster decay of their centerline velocity with down-stream distance. It should be pointed out that, since $b\sim z$, $1/\mu(d\mu/dz)\sim z^{-1}$, i.e., the dilution rate keeps decreasing with downstream distance.

The complete turbulent kinetic energy equation can be found in the literature (e.g., for axisymmetric jets see [5]). The dominant kinetic energy production term is $\overline{uv}\,\partial U/\partial\xi$. Using Eqs. (3), (7), and (13) we can write

$$\left|\frac{\overline{uv}}{U_c^3}\frac{\partial U}{\partial\xi}\right|=c(\exp(-2\xi^2)-\exp(-3\xi^2))\quad\text{(axisymmetric jets)}$$

$$\left|\frac{\overline{uv}}{U_c^3}\frac{\partial U}{\partial\xi}\right|=\frac{\sqrt{\pi}c}{2}\,\xi\exp(-2\xi^2)\mathrm{erf}(\xi)\quad\text{(planar jets)}.$$

The production term has a maximum around $\xi=0.6$ (close to the maximum of the $\overline{uv}$ term) and reduces to zero for large ξ (Fig. 5).

Again, the maxima of the production terms for axisymmetric and planar jets lie at almost the same ξ. The magnitude of the turbulent kinetic energy term for axisymmetric jets is slightly larger than planar jets. The similarity of these terms is due to the fact that both $\overline{uv}$ and $\partial U/\partial\xi$ resemble each other closely for the two cases considered here.

One can derive corresponding expressions for ν_T for the axisymmetric and planar jets using

$$\overline{uv}=-\nu_T\frac{\partial U}{\partial r}, \tag{16}$$

as

$$\frac{\nu_{T_{\text{axisym.}}}}{U_c b}=\frac{c}{4}\,\frac{1-\exp(-\xi^2)}{\xi^2},$$

and

$$\frac{\nu_{T_{\text{planar}}}}{U_c b}=\frac{\sqrt{\pi}c}{8}\,\frac{\mathrm{erf}(\xi)}{\xi}.$$

Because $\nu_T\sim U_c b$ (product of the integral velocity and length scales), we can expect $\nu_{T_{\text{axisym.}}}\sim z^0$ ($b\sim z$, and $U_c\sim z^{-1}$ for axisymmetric jets) and, $\nu_{T_{\text{planar}}}\sim z^{1/2}$ ($b\sim z$, and $U_c\sim z^{-1/2}$ for planar jets), i.e., not only is ν_T a function of radius, it can also be a function of z. Lessen [21] predicted identical z-dependences for ν_T based on the principle of marginal instability. While the streamwise variation of ν_T is well known, ν_T is generally assumed to be independent of ξ, [6–10]. The results presented next indicate that this need not be true.

The eddy viscosity ν_T for the axisymmetric and planar cases are plotted in Fig. 6. ν_T is a maximum at the center of the jet and decays to 0 for large ξ. For the axisymmetric case we find that

$\nu_T(\xi=0)$ is 2.3 times greater than $\nu_T(\xi=\sqrt{2})$. ($\xi=\sqrt{2}$ represents the e^{-2} point of the Gaussian.) For the planar case, this ratio is about 1.7. Townsend [8] also observes that ν_T should diminish as the jet edge is approached because the measured velocity profiles approach zero more rapidly than the profiles calculated on the basis of constant ν_T. Pope [9] states that ν_T is within 15% of the value 0.028 over bulk of the (axisymmetric) jet, and therefore ν_T can be assumed constant, independent of ξ.

Turbulent Plumes

Axisymmetric Plumes. The continuity equation remains the same as Eq. (1) for axisymmetric plumes, whereas a buoyancy term appears in the simplified momentum Eq. (2), [13,14]:

$$V\frac{\partial U}{\partial r}+U\frac{\partial U}{\partial z}+\frac{1}{r}\frac{\partial r\overline{uv}}{\partial r}=g\beta\theta. \tag{17}$$

The $g\beta\theta$ term in Eq. (17) differentiates the plume from the jet. The temperature equation can be obtained starting from

$$V\frac{\partial\theta}{\partial r}+U\frac{\partial\theta}{\partial z}+\frac{\partial\overline{v\theta'}}{\partial r}+\frac{\partial\overline{u\theta'}}{\partial z}+\frac{\overline{v\theta'}}{r}=\gamma\left(\frac{\partial^2\theta}{\partial r^2}+\frac{1}{r}\frac{\partial\theta}{\partial r}+\frac{\partial^2\theta}{\partial z^2}\right),$$

using scaling arguments (similar to jets), to finally arrive at ([13,14])

$$V\frac{\partial\theta}{\partial r}+U\frac{\partial\theta}{\partial z}+\frac{1}{r}\frac{\partial r\overline{v\theta'}}{\partial r}=0. \tag{18}$$

A Gaussian profile is commonly used in the literature to approximate the distributions for velocity and temperature in plumes, [1,2,11,13,14,16]. From similarity considerations, the centerline velocity and temperature for axisymmetric plumes vary, respectively, as $z^{-1/3}$ and $z^{-5/3}$ while the width increases linearly, [6]. Therefore, the streamwise velocity is given by Eq. (3), while the temperature in the plume can be written as

$$\theta(r,z)=\theta_c(z)\exp(-r^2/c_T^2z^2)=\theta_c(z)\exp(-H^2\xi^2), \tag{19}$$

where $c_T\neq c$, i.e., temperature and velocity need not spread at identical rates. In fact $c/c_T=H$ is 1.2 for axisymmetric plumes, [11].

Again, from the continuity Eq. (1) and using the decay rate of the centerline velocity, one can derive

$$\frac{V}{U_c}=\frac{c}{\xi}\left(-\frac{5}{6}+\frac{5}{6}\exp(-\xi^2)+\xi^2\exp(-\xi^2)\right). \tag{20}$$

The plot of V/U_c closely resembles axisymmetric jets—plumes experience outflow near the centerline, and an inflow far away from it. However, the maximum positive V is now just 0.4% of U_c (for $\xi=0.33$), while the maximum negative value of 3.8% lies at $\xi=1.87$ (Fig. 7). The cross-stream velocity changes sign at $\xi=0.595-$ much earlier than for jets. This is due to the presence of buoyancy. In fact, the presence of buoyancy in the plume creates contrasting effects near the center and far away from it when compared to the axisymmetric jet. Buoyancy causes the centerline velocity to decay less slowly than the jet. Consequently, the magnitude of the outflow near the centerline is smaller for the plume resulting in a smaller positive V. Secondly, because buoyancy is continuously increasing the momentum of the plume, there is a larger volume influx from its lateral surface. Hence, larger inflow velocities are seen far away from the centerline. This larger inflow is responsible for greater mixing in plumes. Sreenivas and Prasad [22] have proposed a model based on vortex dynamics to explain the greater entrainment in the plumes. It is again found that the inflow velocity *never* equals αU_c for axisymmetric plumes. The expression for V/U_c for axisymmetric plumes can also be found in [1] and the plot in [1,23].

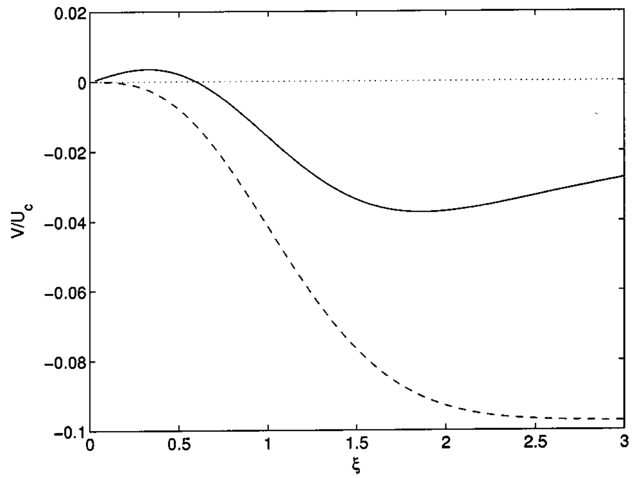

Fig. 7 Cross-stream velocity profiles for plumes (—— axisymmetric plume, -- planar plume)

Similar to axisymmetric jets, for large ξ we can approximate V/U_c as $-5c/6\xi$. The incremental volume flux entrained by the plume is again given by Eq. (5), while our result gives

$$\frac{d\mu}{dz}=\lim_{r\to\infty}-2\pi rV=2\pi r\frac{5c}{6\xi}U_c=2\pi bU_c\frac{5c}{6}.$$

From this, we get $\alpha=5c/6=0.0833$ (using $c=0.100$, [11]). The same value of α was obtained by [11].

Integrating the momentum Eq. (17) using Eqs. (3) and (20) yields

$$\frac{\overline{uv}}{U_c^2}=\frac{c}{\xi}\left(\frac{5}{6}\exp(-\xi^2)-\frac{1}{2}\exp(-2\xi^2)\right)-\frac{g\beta b\theta_c}{2H^2U_c^2\xi}\exp(-H^2\xi^2)+\frac{K}{\xi}$$

where K is a constant of integration. Using the condition that $\overline{uv}$ is bounded at $\xi=0$, we obtain $K=-c/3+g\beta b\theta_c/2H^2U_c^2$, which leads to

$$\frac{\overline{uv}}{U_c^2}=\frac{c}{\xi}\left(\frac{5}{6}\exp(-\xi^2)-\frac{1}{2}\exp(-2\xi^2)-\frac{1}{3}\right)+\frac{g\beta b\theta_c}{2H^2U_c^2\xi}(1-\exp(-H^2\xi^2)). \tag{21}$$

The condition of self-similarity forces $g\beta b\theta_c/U_c^2$ to be a constant, [6], but its value is not directly reported in the literature. However, it can be determined by fitting experimental data. For example, using Beuther et al.'s [24] data we estimate $g\beta b\theta_c/2H^2U_c^2=0.034$. Dai et al.'s [1] data similarly indicates a value of 0.027. Using the latter value, $\overline{uv}<0$ for $\xi\geqslant1.5$, whereas the former value gives $\overline{uv}>0$ for all ξ. A negative Reynolds stress for plumes is unphysical (this is also supported by the data of [1]). Therefore, we use the former value of 0.034 hereafter. Thus,

$$\frac{g\beta b\theta_c}{2H^2U_c^2}=0.034=0.34c\approx\frac{c}{3},$$

implying that $K\approx0$, and $g\beta b\theta_c/U_c^2=0.096$. Setting $K=0$ reduces Eq. (21) to

$$\frac{\overline{uv}}{U_c^2}=\frac{c}{6\xi}(5\exp(-\xi^2)-3\exp(-2\xi^2)-2\exp(-H^2\xi^2)).$$

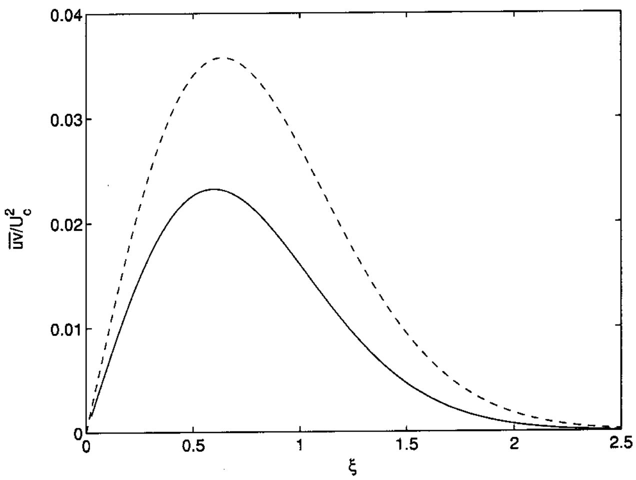

Fig. 8 Reynolds stress profiles for plumes (—— axisymmetric plume, -- planar plume)

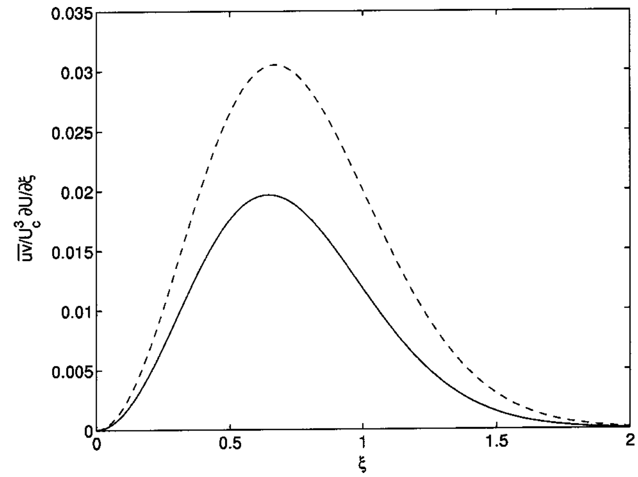

Fig. 10 Dominant kinetic energy production term profiles for plumes (—— axisymmetric plume, -- planar plume)

The behavior of $\overline{uv}$ shown in Fig. 8 looks similar to $\overline{uv}$ of axisymmetric jets. In fact the maxima lie at almost the same ξ ($=0.6$). As can be intuitively expected, Reynolds stress for plumes is larger than jets. Interestingly, this similarity in $\overline{uv}$ for axisymmetric jets and plumes can be inferred by noting that the above expression reduces to Eq. (7) for $H=1$ (although $H=1.2$ for axisymmetric plumes).

From the temperature Eq. (18) and using Eqs. (3), (19), and (20) one can obtain

$$\frac{\overline{v\,\theta'}}{U_c\theta_c}=\frac{5c}{6\xi}(1-\exp(-\xi^2))\exp(-H^2\xi^2). \tag{22}$$

From the plot in Fig. 9 the cross-stream velocity-temperature correlation remains positive for all ξ with a maximum value of 0.026 at $\xi=0.51$.

The production term is obtained as

$$\left|\frac{\overline{uv}}{U_c^3}\frac{\partial U}{\partial\xi}\right|=\frac{c}{3}(5\exp(-2\xi^2)-3\exp(-3\xi^2)$$
$$-2\exp(-(H^2+1)\xi^2)).$$

This has a maximum of 0.020 around $\xi=0.6$ (Fig. 10). This plot matches that of axisymmetric jets quite closely with maxima at almost the same ξ. As expected the production term for the plumes is larger than jets for all ξ.

The dilution rate can be calculated from

$$\frac{1}{\mu}\frac{d\mu}{dz}=\frac{5c}{3b}. \tag{23}$$

Comparing Eqs. (14) and (23), we find that entrainment, and hence dilution rate for axisymmetric plumes is about 1.6 times greater than for axisymmetric jets.

The normalized eddy viscosity can be obtained using Eq. (16) as

$$\frac{\nu_T}{U_cb}=\frac{c}{12\xi^2}(5-3\exp(-\xi^2)-2\exp(-(H^2-1)\xi^2)).$$

Here again the variation with ξ is large. In fact, the ratio of $\nu_T(\xi=0)$ to $\nu_T(\xi=\sqrt{2})>2$ (Fig. 11). In addition, $\nu_T\sim z^{2/3}$.

For plumes, a further assumption of constant (in cross-stream direction) eddy thermal diffusivity, γ_T has been made by the researchers in the past to obtain the functional forms of the similarity functions where

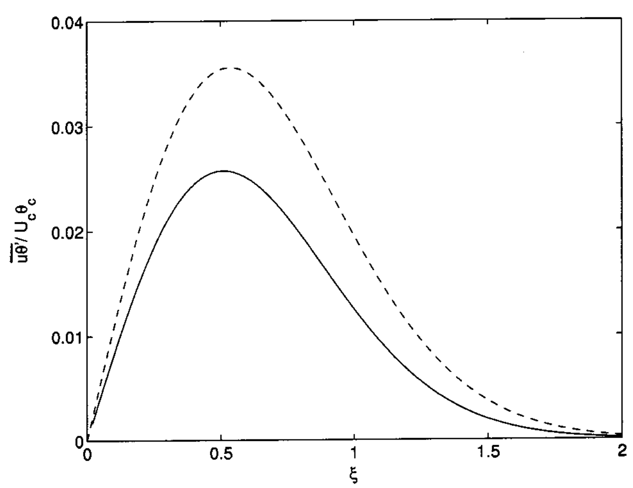

Fig. 9 Velocity-temperature correlation for plumes (—— axisymmetric plume, -- planar plume)

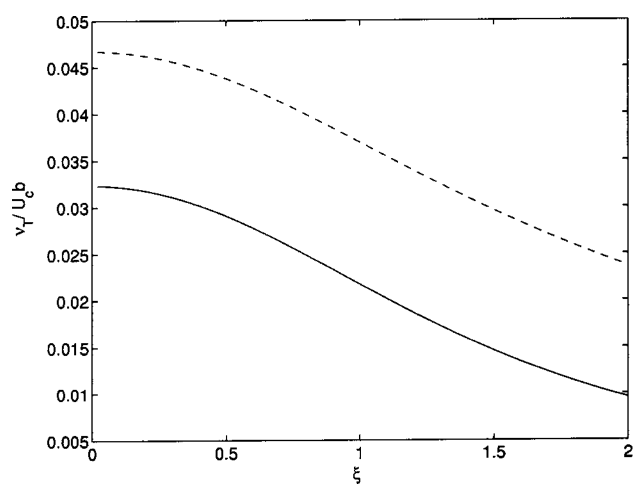

Fig. 11 Cross-stream variation of eddy viscosity for plumes (—— axisymmetric plume, -- planar plume)

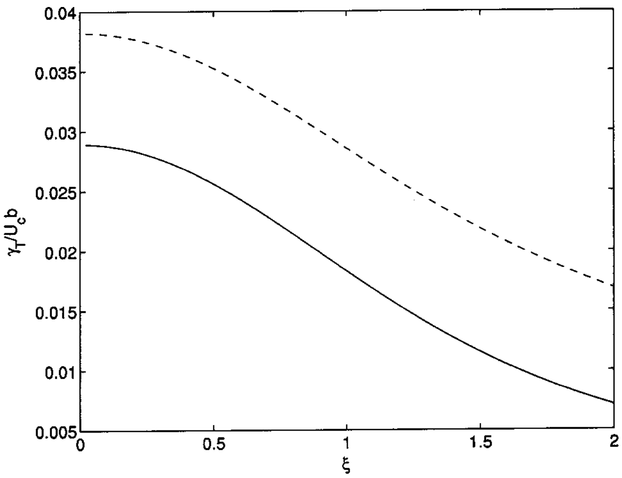

Fig. 12 Cross-stream variation of eddy thermal diffusivity for plumes (—— axisymmetric plume, -- planar plume)

$$\overline{v\,\theta'} = -\gamma_T \frac{\partial \theta}{\partial r}. \tag{24}$$

Our approach provides the radial variation in γ_T (using Eqs. (19) and (22)) as

$$\frac{\gamma_T}{U_c b} = \frac{5c}{12H^2\xi^2}(1-\exp(-\xi^2)).$$

Figure 12 reveals that $\gamma_T/(U_c b)$ has a value of 0.029 at the centerline while it drops to 0.012 for $\xi=\sqrt{2}$, i.e., the radial variation in γ_T is substantial. Moreover, γ_T is a function of downstream distance, i.e., $\gamma_T \sim z^{2/3}$. Knowing the distribution of both ν_T and γ_T we can obtain the turbulent Prandtl number, Pr_T as a function of ξ as

$$\mathrm{Pr}_T = \frac{\gamma_T}{\nu_T} = \frac{5}{H^2}\,\frac{1-\exp(-\xi^2)}{5-3\exp(-\xi^2)-2\exp(-(H^2-1)\xi^2)}.$$

It is interesting to note that unlike ν_T and γ_T, Pr_T is independent of the spread rate and z. Moreover, Pr_T is not such a strong function of radial position as ν_T and γ_T. Pr_T varies from 0.9 at the centerline to 0.8 at $\xi=\sqrt{2}$ (Fig. 13). Physical arguments can be used to show that $\mathrm{Pr}_T \approx 1$, [25], and our result is in good agreement.

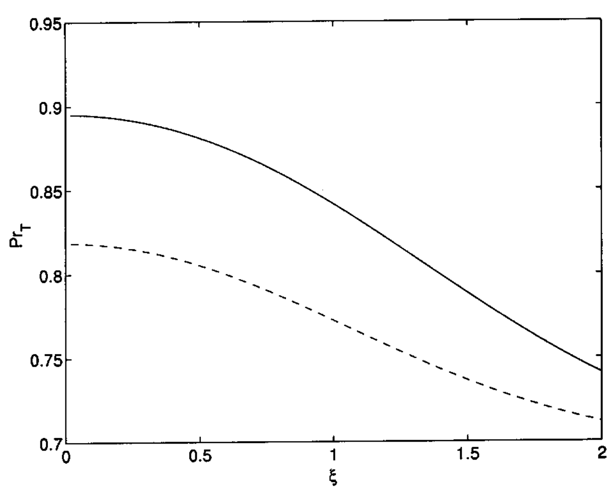

Fig. 13 Cross-stream variation of turbulent Prandtl number for plumes (—— axisymmetric plume, -- planar plume)

Planar Plumes. The continuity equation for planar plumes is the same as for planar jets (Eq. (8)), while the momentum equation can be derived by adding the buoyancy term to the planar jet momentum equation, [6],

$$V\frac{\partial U}{\partial x} + U\frac{\partial U}{\partial z} + \frac{\partial \overline{uv}}{\partial x} = g\beta\theta. \tag{25}$$

The temperature equation in the self-similar regime is given by ([6])

$$V\frac{\partial \theta}{\partial x} + U\frac{\partial \theta}{\partial z} + \frac{\partial \overline{v\,\theta'}}{\partial x} = 0. \tag{26}$$

Here the centerline temperature varies as z^{-1}, while it is interesting to note that the centerline velocity does not change downstream, [6], i.e., presence of buoyancy prevents the decay of the centerline velocity. This has an interesting consequence for the cross-stream velocity, expressed mathematically as

$$\frac{V}{U_c} = \frac{c}{2}(2\xi\exp(-\xi^2) - \sqrt{\pi}\,\mathrm{erf}(\xi)).$$

Unlike axisymmetric plumes, we find that planar plumes do not experience an outflow near the centerline; V/U_c is small for $\xi<0.54$ (less than 10% of its asymptotic value of 0.098) and remains negative throughout, i.e., the flow is always towards the axis (Fig. 7). Qualitatively the plot is similar to planar jets. Buoyancy causes planar plumes to entrain more than planar jets like their axisymmetric counterparts.

Similar to planar jets, we can obtain the coefficient of entrainment as

$$\alpha = \frac{\sqrt{\pi}c}{2}.$$

Using $c=0.11$, [16], we obtain $\alpha=0.0975$.

The Reynolds stress is given by

$$\frac{\overline{uv}}{U_c^2} = \frac{\sqrt{\pi}c}{2}\left(\mathrm{erf}(\xi)\exp(-\xi^2) - \frac{\mathrm{erf}(\sqrt{2}\xi)}{\sqrt{2}}\right) + \frac{\sqrt{\pi}g\beta b\theta_c}{2HU_c^2}\mathrm{erf}(H\xi). \tag{27}$$

Note that the constant of integration is zero in Eq. (27), and for similarity to exist $g\beta b\theta_c/U_c^2$ should be a universal constant, [6]. The experimental data of Ramaprian and Chandrasekhara [16] indicates $H=1.2$ (identical to axisymmetric plumes). We estimate the value of $\sqrt{\pi}g\beta b\theta_c/2HU_c^2$ (denoting this by C) as 0.069 which gives $\overline{uv}_{\max}/U_c^2=0.036$ at $\xi=0.63$. (The maximum value is very close to the value of 0.035 predicted by Malin and Spalding [26]). For Ramaprian and Chandrasekhara's [16] data we obtain $C=0.062$, but we find that $\overline{uv}$ becomes negative for $\xi>1.6$. As in the case of axisymmetric plumes, $\overline{uv}$ should remain positive for all ξ (this is also supported by the data of [16]). Hence, we will use $C=0.069$ to obtain

$$\frac{\sqrt{\pi}g\beta b\theta_c}{2HU_c^2} = 0.069 = 0.71\frac{\sqrt{\pi}c}{2} \approx \frac{\sqrt{\pi}c}{2}\,\frac{1}{\sqrt{2}},$$

and $g\beta b\theta_c/U_c^2=0.093$ which is very close to the value for axisymmetric plumes. Equation (27) can then be simplified to (see Fig. 8)

$$\frac{\overline{uv}}{U_c^2} = \frac{\sqrt{\pi}c}{2}\left(\mathrm{erf}(\xi)\exp(-\xi^2) - \frac{\mathrm{erf}(\sqrt{2}\xi)}{\sqrt{2}} + \frac{\mathrm{erf}(H\xi)}{\sqrt{2}}\right).$$

While it is known that $H=1.2$, an interesting result is obtained by substituting $H=\sqrt{2}$ in the above expression. Then, it is seen that $\overline{uv}$ for planar plumes is twice that of planar jets (Eq. 13).

The velocity-temperature correlation for planar plumes is given by

$$\frac{\overline{v\theta'}}{U_c\theta_c}=\frac{\sqrt{\pi}c}{2}\operatorname{erf}(\xi)\exp(-H^2\xi^2).$$

As for axisymmetric plumes, the velocity-temperature correlation is also positive with a maximum of 0.035 at $\xi=0.53$ (Fig. 9). Note that for both axisymmetric and planar plumes, the maximum value of $\overline{v\theta'}$ is to the left of the maximum for $\overline{uv}$.

We can obtain the production term as

$$\left|\frac{\overline{uv}}{U_c^3}\frac{\partial U}{\partial \xi}\right|=\sqrt{\pi}c\left(\xi\operatorname{erf}(\xi)\exp(-2\xi^2)-\frac{\xi\operatorname{erf}(\sqrt{2}\xi)\exp(-\xi^2)}{\sqrt{2}}+\frac{\xi\operatorname{erf}(H\xi)\exp(-\xi^2)}{\sqrt{2}}\right).$$

As for jets and axisymmetric plumes, this term has a maximum value around $\xi=0.6$ (Fig. 10). In fact, the maximum lies at almost the same location as the maximum of Reynolds stresses. It should be pointed out that unlike for jets, the production term for planar plumes is larger than their axisymmetric counterparts.

The dilution rate for planar plumes can be obtained as

$$\frac{1}{\mu}\frac{d\mu}{dz}=\frac{c}{b}. \tag{28}$$

As expected, the dilution rate of planar plumes is higher than planar jets (compare Eqs. (15) with (28)). Interestingly, it is equal to the dilution rate of axisymmetric jets (Eqs. (14) and (28)).

Once again, we can derive expressions for ν_T, γ_T, and Pr_T and question the validity of assigning constant cross-stream values to them.

$$\frac{\nu_T}{U_cb}=\frac{\sqrt{\pi}c}{4\xi\exp(-\xi^2)}\left(\operatorname{erf}(\xi)\exp(-\xi^2)-\frac{\operatorname{erf}(\sqrt{2}\xi)}{\sqrt{2}}+\frac{\operatorname{erf}(H\xi)}{\sqrt{2}}\right),$$

$$\frac{\gamma_T}{U_cb}=\frac{\sqrt{\pi}c}{4H^2\xi}\operatorname{erf}(\xi),$$

$$\mathrm{Pr}_T=\frac{1}{H^2}\frac{\sqrt{2}\operatorname{erf}(\xi)\exp(-\xi^2)}{\sqrt{2}\operatorname{erf}(\xi)\exp(-\xi^2)-\operatorname{erf}(\sqrt{2}\xi)+\operatorname{erf}(H\xi)}.$$

Turbulent eddy viscosity and thermal diffusivity are plotted in Figs. 11 and 12, respectively. Both ν_T and $\gamma_T\sim z$. Pr_T has a maximum value of 0.82 (at the centerline) while it drops to 0.74 for $\xi=\sqrt{2}$ (Fig. 13). It is again reassuring to note that $\mathrm{Pr}_T\approx 1$ as predicted by physical arguments, [25].

Turbulent Wakes

Axisymmetric Wakes. Unlike jets and plumes, wakes have a nonlinear spread rate. The continuity equation for axisymmetric wakes remains the same as Eq. (1), while the momentum equation can be derived as for axisymmetric jets. However, here u'/U_c is of order unity, i.e., the velocity fluctuations are of the order of the velocity defect, [6]. This simplifies the momentum equation further:

$$U\frac{\partial U}{\partial z}+\frac{1}{r}\frac{\partial r\overline{uv}}{\partial r}=0. \tag{29}$$

It is interesting to note that V does not appear in the streamwise momentum equation. This is because in the momentum equation $V\partial U/\partial r=\mathcal{O}(U_c^2/L)$, while $U\partial U/\partial z=\mathcal{O}(U_0U_c/L)$; since $U_c/U_0=\mathcal{O}(b/L)$, the former can be discarded.

Using a Gaussian profile for the velocity defect, the streamwise velocity is given by

$$U(r,z)=U_0-U_c(z)\exp(-r^2/b^2)=U_0-U_c(z)\exp(-\xi^2). \tag{30}$$

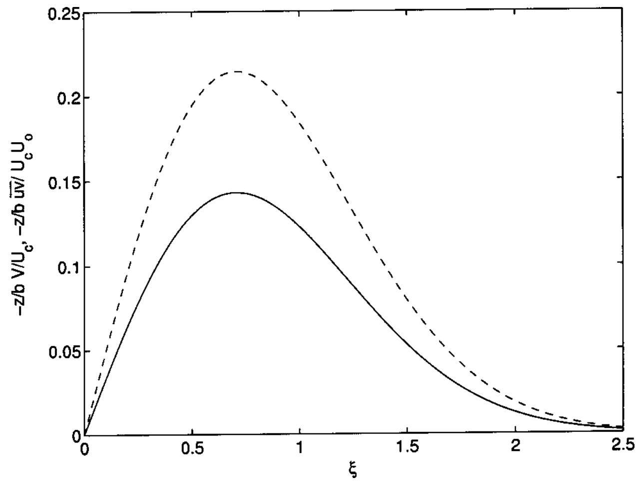

Fig. 14 Cross-stream velocity and Reynolds stress profiles for wakes (—— axisymmetric wake, -- planar wake)

In the self-similar region U_c decreases as $z^{-2/3}$, while b increases as $z^{1/3}$, [6]. Keeping these in mind, we can obtain V from the continuity Eq. (1) as

$$\frac{V}{U_c}=-\frac{b\xi}{3z}\exp(-\xi^2). \tag{31}$$

As for planar plumes, inflow occurs for all ξ with a maximum at $\xi=0.71$.

Reynolds stress can be obtained using Eqs. (29) and (30) as

$$\frac{\overline{uv}}{U_c^2}=\frac{b}{12z\xi}\left(1-\exp(-2\xi^2)+2\xi^2\exp(-2\xi^2)-\frac{4U_0}{U_c}\xi^2\exp(-\xi^2)\right). \tag{32}$$

It should be mentioned that in this case the integration constant is nonzero (actually $K=b/12z\xi$). It is not possible to plot Eq. (32) without knowing U_0/U_c. However, since $U/U_0=\mathcal{O}(1)$, one can simplify the momentum equation by replacing $U\partial U/\partial z$ by $U_0\partial U/\partial z$, [6], to obtain:

$$U_0\frac{\partial U}{\partial z}+\frac{1}{r}\frac{\partial r\overline{uv}}{\partial r}=0. \tag{33}$$

On comparing Eqs. (1) and (33), we can see that they are identical ($\overline{uv}/U_0$ replaces V). Hence it is not surprising to see

$$\frac{\overline{uv}}{U_0U_c}=-\frac{b\xi}{3z}\exp(-\xi^2), \tag{34}$$

which is exactly the same expression as for V/U_c. It should, however, be noted that $\overline{uv}$ has been normalized with U_0U_c and not U_c^2. $\overline{uv}/U_0U_c$ and V/U_c are plotted in Fig. 14.

We will use the expression for $\overline{uv}$ given by Eq. (32) to obtain the production term and the radial variation in turbulent eddy viscosity as

$$\left|\frac{\overline{uv}}{U_c^3}\frac{\partial U}{\partial \xi}\right|=\frac{b}{6z}\left(1-\exp(-2\xi^2)+2\xi^2\exp(-2\xi^2)-\frac{4U_0}{U_c}\xi^2\exp(-\xi^2)\right)\exp(-\xi^2),$$

$$\frac{\nu_T}{U_c b} = \frac{b}{24z\xi^2 \exp(-\xi^2)}\left(1 - \exp(-2\xi^2) + 2\xi^2 \exp(-2\xi^2) - \frac{4U_0}{U_c}\xi^2 \exp(-\xi^2)\right).$$

Planar Wakes. The continuity equation for planar wakes is given by Eq. (8) while the momentum equation is, [6],

$$U\frac{\partial U}{\partial z} + \frac{\partial \overline{uv}}{\partial x} = 0. \tag{35}$$

U_c varies as $z^{-1/2}$, while b increases as $z^{1/2}$ for planar wakes, [6,21]. Integrating the continuity Eq. (8) gives

$$\frac{V}{U_c} = -\frac{b\xi}{2z}\exp(-\xi^2). \tag{36}$$

Comparing Eqs. (31) and (36), we see that the inward velocity is very similar. However, the decay with z is slightly different for the two cases.

Reynolds stress can be obtained from the momentum Eq. (35) using Eq. (30):

$$\frac{\overline{uv}}{U_c^2} = \frac{b}{16z}\left(-4\xi \exp(-2\xi^2) + \sqrt{2\pi}\,\mathrm{erf}(\sqrt{\pi}\xi) - \frac{8U_0}{U_c}\xi \exp(-\xi^2)\right).$$

The production term is

$$\left|\frac{\overline{uv}}{U_c^3}\frac{\partial U}{\partial \xi}\right| = \frac{b\xi}{8z}\left(-4\xi \exp(-2\xi^2) + \sqrt{2\pi}\,\mathrm{erf}(\sqrt{\pi}\xi) - \frac{8U_0}{U_c}\xi \exp(-\xi^2)\right)\exp(-\xi^2).$$

ν_T can be obtained as

$$\frac{\nu_T}{U_c b} = \frac{b}{32z\xi \exp(-\xi^2)}\left(-4\xi \exp(-2\xi^2) + \sqrt{2\pi}\,\mathrm{erf}(\sqrt{\pi}\xi) - \frac{8U_0}{U_c}\xi \exp(-\xi^2)\right).$$

Simplifying the momentum equation as was done with axisymmetric wakes, and using it to obtain the simplified Reynolds stress

$$\frac{\overline{uv}}{U_0 U_c} = -\frac{b\xi}{2z}\exp(-\xi^2), \tag{37}$$

which, as expected, is the same expression as for V/U_c for planar wakes (Fig. 14).

It is not possible to compare the production terms for the axisymmetric and planar wakes because U_0 is unknown. However, if we use the simplified expressions for the Reynolds stress (Eqs. (34) and (37)), we can write the productions terms as

$$\frac{\overline{uv}}{U_0 U_c^2}\frac{\partial U}{\partial \xi} = \frac{2b}{3}\frac{\xi^2 \exp(-2\xi^2)}{z} \quad \text{(axisymmetric wakes)}$$

$$\frac{\overline{uv}}{U_0 U_c^2}\frac{\partial U}{\partial \xi} = \frac{b\xi^2 \exp(-2\xi^2)}{z} \quad \text{(planar wakes)}.$$

These two terms differ just by a constant.

The simplified expressions for ν_T (using Eqs. (16), (30), (34), and (37)) are

$$\nu_{T_{\text{axisym.}}} = -\frac{U_0 b^2}{6z},$$

$$\nu_{T_{\text{planar}}} = -\frac{U_0 b^2}{4z}.$$

Since U_0 is invariant with z, we obtain $\nu_{T_{\text{axisym. wake}}} \sim z^{-1/3}$ while $\nu_{T_{\text{planar wake}}} \sim z^0$, in agreement with Lessen's predictions, [21]. Remarkably, the dependence of ν_T on ξ disappears for wakes.

Conclusions

A comprehensive analysis has been conducted for six standard cases (axisymmetric and planar jets, plumes, and wakes). Expressions for cross-stream velocity, Reynolds stress, and turbulent kinetic energy production terms are derived for these cases assuming a Gaussian streamwise velocity distribution. The plots are compared amongst themselves and provide several insights.

1 Expressions for cross-stream velocity indicate outflow for jets and axisymmetric plumes near the axis, while inflow occurs in the far field. Planar plumes do not experience any such outflow. Outflow of fluid near the axis is a natural consequence of the decay of the centerline velocity with downstream distance (and not because of the assumed Gaussian velocity profile). The decay rates of axisymmetric jets, planar jets, and axisymmetric plumes are, respectively, z^{-1}, $z^{-1/2}$, $z^{-1/3}$, while the radial extents of outflow are $r/b \leq 1.12$, 0.99, 0.59. Moreover, the decay rate for planar plumes varies as z^0 and these do not experience any outflow. Thus, a higher decay rate correlates with a larger radial extent of outflow. See Agrawal et al. [20] for more discussion on the coupling between the decay of the centerline velocity and the radial extent of the outflow.

2 Expressions for the entrainment coefficients of planar jets and plumes are developed along the lines of their axisymmetric counterparts. It is found that for planar jets and plumes $V_e = \alpha U_c$; this is, however, not true for axisymmetric cases. Hence, contrary to conventional belief, the entrainment velocity *should not* be equated to αU_c for axisymmetric jets and plumes.

3 The value of the universal constant $g\beta b\theta_c/U_c^2$ is estimated as 0.096 and 0.093 for axisymmetric and planar plumes, respectively.

4 Reynolds stress and the dominant turbulent kinetic energy production term for jets and plumes are qualitatively the same with a maximum around $\xi = 0.6$. Magnitudes for jets and axisymmetric plumes are nearly the same. These are much smaller than for planar plumes.

5 Unlike plumes and jets, the normalized cross-stream velocity and Reynolds stresses for wakes are functions of downstream distance. In addition, the turbulent kinetic energy production term for axisymmetric and planar wakes has the same cross-stream distribution.

6 Cross-stream variations for ν_T, γ_T, and Pr_T are shown to be significant, therefore, the use of constant values of ν_T and γ_T in the cross-stream direction is unjustified. Pr_T is found to lie between 0.9 and 0.7 for axisymmetric and planar plumes.

7 Our analysis reveals that the eddy viscosity is independent of the cross-stream coordinate for axisymmetric and planar wakes.

Acknowledgments

This work was supported by National Science Foundation, under grant NSF-ATM-9714810. We thank Prof. Pablo Huq of the College of Marine Studies, University of Delaware, for encouraging us to undertake this study and helpful discussions.

Nomenclature

b = width (defined as $U(b)/U_c = e^{-1}$ for jets and plumes, and $(U_0 - U(b))/U_c = e^{-1}$ for wakes)
c = spread rate $= db/dz$
c_T = spread rate for temperature
d = diameter of the nozzle
g = acceleration due to gravity

H = c/c_T
K = constant of integration
L = downstream distance scale
p = time-averaged pressure
Pr_T = turbulent Prandtl number
r = cross-stream coordinate used for axisymmetric case
T = temperature
T' = fluctuating temperature
T_0 = ambient fluid temperature (assumed constant)
T_c = time-averaged centerline temperature
u, v = fluctuating components of velocity
u' = fluctuating velocity scale
U = time-averaged streamwise velocity
U_0 = free stream velocity
U_c = time-averaged centerline velocity (for wakes—velocity defect at the centerline)
V = time-averaged cross-stream velocity
V_e = time-averaged entrainment velocity
x = cross-stream coordinate used for planar case
z = coordinate along the axis
α = coefficient of entrainment
β = coefficient of thermal expansion
γ = thermal diffusivity
γ_T = turbulent thermal diffusivity
θ = $T-T_0$
θ' = $T'-T_0$
θ_c = T_c-T_0
μ = volume flux
ν_T = eddy viscosity
ξ = nondimensional cross-stream coordinate ($=r/b$ for axisymmetric case, $=x/b$ for planar case. See Fig. 2)
ρ = density

References

[1] Dai, Z., Tseng, L. K., and Faeth, G. M., 1995, ‘‘Velocity Statistics of Round, Fully Developed, Buoyant Turbulent Plumes,’’ ASME J. Heat Transfer, **117**, pp. 138–145.
[2] George, W. K., Alpert, R. L., and Tamanini, F., 1977, ‘‘Turbulence Measurements in an Axisymmetric Buoyant Plume,’’ Int. J. Heat Mass Transfer, **20**, pp. 1145–1153.
[3] Bhat, G. S., and Narasimha, R., 1996, ‘‘A Volumetrically Heated Jet: Large Eddy Structure and Entrainment Characteristics,’’ J. Fluid Mech., **325**, pp. 303–330.
[4] Hussein, H. J., Capp, S. P., and George, W. K., 1994, ‘‘Velocity Measurements in a High Reynolds Number, Momentum-Conserving Axisymmetric Turbulent Jet,’’ J. Fluid Mech., **258**, pp. 31–75.
[5] Wygnanski, I., and Fiedler, H., 1969, ‘‘Some Measurements in a Self-Preserving Jet,’’ J. Fluid Mech., **38**, pp. 577–612.
[6] Tennekes, H., and Lumley, J. L., 1972, *A First Course in Turbulence*, MIT Press, Cambridge, MA, pp. 127–142.
[7] White, F. M., 1974, *Viscous Fluid Flow*, McGraw-Hill, New York, pp. 508–510.
[8] Townsend, A. A., 1976, *The Structure of Turbulent Shear Flow*, Cambridge Univ. Press, Cambridge, UK, pp. 188–219.
[9] Pope, S. B., 2000, *Turbulent Flows*, Cambridge Univ. Press, Cambridge, UK, pp. 102–120.
[10] Lesieur, M., 1990, *Turbulence in Fluids*, Kluwer, Dordrecht, The Netherlands, pp. 120–126.
[11] Turner, J. S., 1986, ‘‘Turbulent Entrainment: The Development of the Entrainment Assumption, and Its Application to Geophysical Flows,’’ J. Fluid Mech., **173**, pp. 431–471.
[12] List, E. J., 1982, ‘‘Turbulent Jets and Plumes,’’ Annu. Rev. Fluid Mech., **14**, pp. 189–212.
[13] Chen, C. J., and Rodi, W., 1980, *Vertical Turbulent Buoyant Jets—A Review of Experimental Data*, Pergamon Press, Oxford, UK, pp. 11–12.
[14] Gebhart, B., Jaluria, Y., Mahajan, R. L., and Sammakia, B., 1988, *Buoyancy-Induced Flows and Transport*, Hemisphere, Washington, DC, pp. 661–663.
[15] Ramaprian, B. R., and Chandrasekhara, M. S., 1985, ‘‘LDA Measurements in Plane Turbulent Jets,’’ ASME J. Fluids Eng., **107**, pp. 264–271.
[16] Ramaprian, B. R., and Chandrasekhara, M. S., 1989, ‘‘Measurements in Vertical Plane Turbulent Plumes,’’ ASME J. Fluids Eng., **111**, pp. 69–77.
[17] Agrawal, A., and Prasad, A. K., 2002, ‘‘Properties of Vortices in the Self-Similar Turbulent Jet,’’ Exp. Fluids, **33**, pp. 565–577.
[18] Gutmark, E., and Wygnanski, I., 1976, ‘‘The Planar Turbulent Jet,’’ J. Fluid Mech., **73**, pp. 465–495.
[19] Narasimha, R., 2001, private communication.
[20] Agrawal, A., Sreenivas, K. R., and Prasad, A. K., 2003, ‘‘Velocity and Temperature Measurements in an Axisymmetric Jet With Cloud-Like Off-Source Heating,’’ Int. J. Heat Mass Transfer, to appear.
[21] Lessen, M., 1978, ‘‘On the Power Laws for Turbulent Jets, Wakes and Shearing Layers and Their Relationship to the Principal of Marginal Instability,’’ J. Fluid Mech., **88**, pp. 535–540.
[22] Sreenivas, K. R., and Prasad, A. K., 2000, ‘‘Vortex-Dynamics Model for Entrainment in Jets and Plumes,’’ Phys. Fluids, **12**, pp. 2101–2107.
[23] Lumley, J. L., 1971, ‘‘Explanation of Thermal Plume Growth Rates,’’ Phys. Fluids, **14**, pp. 2537–2538.
[24] Beuther, P. D., Capp, S. P., and George, W. K., Jr., 1979, ‘‘Momentum and Temperature Balance Measurements in an Axisymmetric Turbulent Plumes,’’ ASME Paper No. 79-HT-42.
[25] Kays, W. M., and Crawford, M. E., 1980, *Convective Heat and Mass Transfer*, McGraw-Hill, New York, pp. 267–268.
[26] Malin, M. R., and Spalding, D. B., 1984, ‘‘The Prediction of Turbulent Jets and Plumes by Use of the k-ω Model of Turbulence,’’ PhysicoChemical Hydrodynamics, **5**, pp. 153–198.